than traditionally designed shapers of comparable duration. Computer simulations of a single-mode system demonstrated the advantages of the new shapers. MACE results collected aboard the Space Shuttle Endeavor demonstrated the shapers' vibration-reducing ability on real structures.

Acknowledgments

We would like to thank members of MIT's SERC lab for implementing our experiments on the MACE program. Support for this work was provided by Convolve, Inc. under NASA contract NAS5-32034 and the Office of Naval Research Fellowship Program. The methods described in this paper are covered under United States patent #4,916,635; April 10, 1990, and other patents pending. Commercial use of these methods requires written permission from the Massachusetts Institute of Technology.

References

Bhat, S. P., and Miu, D. K., 1990, "Precise Point-to-Point Positioning Control of Flexible Structures," ASME JOURNAL OF DYNAMIC SYSTEMS, MEASUREMENT, AND CONTROL, Vol. 112(4), pp. 667–674.

Jones, S. D., and Ulsoy, A. G., 1994, "Control Input Shaping for Coordinate Measuring Machines," American Control Conference, Baltimore, MD, Vol. 3, pp. 2899–2903.

Magee, D. P., and Book, W. J., 1994, "Filtering Schilling Manipulator Commands to Prevent Flexible Structure Vibration," American Control Conference, Baltimore, MD, pp. 2538–42.

Seth, N., Rattan, K. S., and Brandstetter, R. W., 1993, "Vibration Control of a Coordinate Measuring Machine," IEEE Conference on Control Applications, Dayton, OH, pp. 368–73.

Singer, N. C., 1989, "Residual Vibration Reduction in Computer Controlled Machines," Technical Report MIT Artificial Intelligence Laboratory Technical Report Number AITR-1030, MIT Artificial Intelligence Lab.

Singer, N. C., and Seering, W. P., 1990, "Preshaping Command Inputs to Reduce System Vibration," ASME JOURNAL OF DYNAMIC SYSTEMS, MEASUREMENT, AND CONTROL, Vol. 112, Mar., pp. 76–82.

Singh, T., and Heppler, G. R., 1993, "Shaped Input Control of a System With Multiple Modes," ASME JOURNAL OF DYNAMIC SYSTEMS, MEASUREMENT, AND CONTROL, Vol. 115, Sept., pp. 341–437.

Singh, T., and Vadali, S. R., 1994, "Robust Time-Optimal Control: A Frequency Domain Approach," *AIAA Journal of Guidance, Control and Dynamics,* Vol. 17(2), pp. 346–353.

Singhose, W., Seering, W., and Singer, N., 1994, "Residual Vibration Reduction Using Vector Diagrams to Generate Shaped Inputs," ASME *Journal of Mechanical Design,* Vol. 116, June, pp. 654–659.

Smith, O. J. M., 1958, *Feedback Control Systems,* McGraw-Hill, New York, pp. 331–345.

Tuttle, T. D., and Seering, W. P., 1994, "A Zero-placement Technique for Designing Shaped Inputs to Suppress Multiple-mode Vibration," American Control Conference, Baltimore, MD, Vol. 3, pp. 2533–2537.

Tuttle, T. D., and Seering, W. P., 1996, "Vibration Reduction in Flexible Space Structures Using Input Shaping on MACE: Mission Results," IFAC World Congress, San Francisco, CA.

Vibration Controllability of 3D Flexible Manipulators

S. López-Linares,[1] A. Konno,[2] and M. Uchiyama[3]

Structural vibrations of flexible robots are not always fully controllable in all the workspace. In some cases, there exist configurations where the actuators cannot affect some of the vibration modes, and thus cannot control their vibrations. This problem has been neglected in the case of the one-link and two-link planar manipulators; however, it must be dealt with in depth when trying to control a 3D flexible robot. This paper discusses the vibration controllability of flexible manipulators. Vibration uncontrollable configurations are estimated both by the minimum singular values of the controllability matrix and the closed-loop behavior. A 2-link 3-joint prototype flexible manipulator is used for a case study, and the uncontrollable configurations of the manipulator are found.

1 Introduction

A great deal of interest has been put lately to study the flexible manipulators. They are foreseen as the new generation of industrial robots with lower ratio of arm weight to payload weight, higher safety, and higher power efficiency.

Research has concentrated mainly on modeling (Book, 1984 and Siciliano and Book, 1988), inverse dynamics (Bayo et al., 1984), vibration suppression of the one-link (Cannon and Schmitz, 1984; Sakawa et al., 1985; Kotnik et al., 1988; López-Linares et al., 1991) and two-link (Fukuda, 1985; Khorrami and Jain, 1992) planar flexible manipulators, and trajectory tracking (Uchiyama et al., 1990).

There is very little literature on controllability of flexible manipulators. Balas discussed about the controllability of planar case (Balas, 1978). He divided the infinite vibration modes into the controlled modes and residual (uncontrolled) modes. In this paper, we do not consider the effect of the residual modes.

Tosunoglu et al. (1992) have considered the configuration dependency of the controllability, but do not take into account the vibration modes in their study. Konno et al. (1994) take into account the vibration modes and find that, in the case of 3D manipulators, there exist configurations where some of the vibration modes cannot be controlled due to the fact that they are inaccessible by the actuators. In this paper, we give a method to study the uncontrollable configurations of a general flexible manipulator.

First, in Section 2 we make some assumptions to simplify the dynamic equation and we form the controllability matrix. Then, in Section 3, we present the control method that was used in the experiments with FLEBOT II (the 2-link 3-joint flexible robot built at Tohoku University). Finally, Section 4 shows the results of the numerical simulation of the robot, introducing the concept of controllable subspaces, and Section 5 confirms the simulations with experiments.

2 Vibration Controllability Matrix

Ignoring the structural damping, the dynamic equation of a flexible manipulator can be written as

$$\begin{bmatrix} \mathbf{M}_{11}(\boldsymbol{\theta}, \mathbf{e}) & \mathbf{M}_{12}(\boldsymbol{\theta}, \mathbf{e}) \\ \mathbf{M}_{21}(\boldsymbol{\theta}, \mathbf{e}) & \mathbf{M}_{22}(\boldsymbol{\theta}, \mathbf{e}) \end{bmatrix} \begin{bmatrix} \ddot{\boldsymbol{\theta}} \\ \ddot{\mathbf{e}} \end{bmatrix} + \begin{bmatrix} \mathbf{h}_1(\boldsymbol{\theta}, \dot{\boldsymbol{\theta}}, \mathbf{e}, \dot{\mathbf{e}}) \\ \mathbf{h}_2(\boldsymbol{\theta}, \dot{\boldsymbol{\theta}}, \mathbf{e}, \dot{\mathbf{e}}) \end{bmatrix} + \begin{bmatrix} 0 & 0 \\ 0 & \mathbf{K}_{22} \end{bmatrix} \begin{bmatrix} \boldsymbol{\theta} \\ \mathbf{e} \end{bmatrix} + \begin{bmatrix} \mathbf{g}_1(\boldsymbol{\theta}, \mathbf{e}) \\ \mathbf{g}_2(\boldsymbol{\theta}, \mathbf{e}) \end{bmatrix} = \begin{bmatrix} \boldsymbol{\tau} \\ \mathbf{0} \end{bmatrix} \quad (1)$$

or in a more compact form

$$\mathbf{M}(\mathbf{q})\ddot{\mathbf{q}} + \mathbf{h}(\mathbf{q}, \dot{\mathbf{q}}) + \mathbf{K}\mathbf{q} + \mathbf{g}(\mathbf{q}) = \mathbf{L}\boldsymbol{\tau} \quad (2)$$

where

$\mathbf{q} = \begin{bmatrix} \boldsymbol{\theta} \\ \mathbf{e} \end{bmatrix}$ is the vector of coordinates
$\boldsymbol{\theta}$ are the joint rotations (dimension n)
$\mathbf{e}$ are the elastic deflections (dimension m),
$\boldsymbol{\tau}$ is the vector of applied torques (dimension n),
$\mathbf{M}(\mathbf{q})$ is the inertia matrix,
$\mathbf{h}(\mathbf{q}, \dot{\mathbf{q}})$ is the vector of centrifugal and Coriolis forces,

[1] Robotics Laboratory, C.E.I.T., San Sebastián, Spain. Dr. López-Linares is currently working at IBERINCO, Gardoqui 8, 48008 Bilbao, Spain.

[2] Department of Mechano-Informatics, University of Tokyo, Japan.

[3] Department of Aeronautics and Space Eng., Tohoku University, Japan.

Contributed by the Dynamic Systems and Control Division of THE AMERICAN SOCIETY OF MECHANICAL ENGINEERS. Manuscript received by the DSCD February 29, 1996. Associate Technical Editor: B. Siciliano.

$\mathbf{K}$ is a constant matrix of elasticity related only to the elastic coordinates,

$\mathbf{g}(\mathbf{q})$ is the vector of gravity forces, and

$\mathbf{L}$ is a constant matrix to transform the applied torques to the generalized forces of the system

$$\mathbf{L} = \begin{bmatrix} \mathbf{I}_{n\times n} \\ \mathbf{0} \end{bmatrix}$$

The upper part of the dynamic equation is related to the overall motion of the robot and the lower part is related to the elastic deformations. In the case of $\ddot{\boldsymbol{\theta}} = \dot{\boldsymbol{\theta}} = \mathbf{0}$ and $\ddot{\mathbf{e}} = \dot{\mathbf{e}} = \mathbf{0}$ we obtain the static displacement $\mathbf{e}_0$ produced by gravity in the structure of the robot as

$$\mathbf{K}_{22}\mathbf{e}_0 + \mathbf{g}_2(\boldsymbol{\theta}, \mathbf{e}_0) = 0 \tag{3}$$

In order to study this complex system we are going to make two assumptions:

- First, we will only consider the stationary behaviour neglecting centrifugal and Coriolis forces $\mathbf{h}(\mathbf{q}, \dot{\mathbf{q}}) = \mathbf{0}$, as well as the time dependence of the inertia matrix $\dot{\mathbf{M}}(\mathbf{q}) = \mathbf{0}$
- Second, we will assume that the influence of elastic deformations $\mathbf{e}$ in the inertia matrix and the gravity term is small:

$$\mathbf{M}(\mathbf{q}) \approx \mathbf{M}(\boldsymbol{\theta}), \quad \mathbf{g}(\mathbf{q}) \approx \mathbf{g}(\boldsymbol{\theta})$$

Then, substracting Eq. (3) from the lower part of Eq. (1), it is possible to balance the effect of gravity at any configuration $\boldsymbol{\theta}$. The approximated dynamic equation of the flexible arm is

$$\begin{bmatrix} \mathbf{M}_{11}(\boldsymbol{\theta}) & \mathbf{M}_{12}(\boldsymbol{\theta}) \\ \mathbf{M}_{21}(\boldsymbol{\theta}) & \mathbf{M}_{22}(\boldsymbol{\theta}) \end{bmatrix} \begin{bmatrix} \ddot{\boldsymbol{\theta}} \\ \Delta\ddot{\mathbf{e}} \end{bmatrix} + \begin{bmatrix} \mathbf{0} & \mathbf{0} \\ \mathbf{0} & \mathbf{K}_{22} \end{bmatrix} \begin{bmatrix} \boldsymbol{\theta} \\ \Delta\mathbf{e} \end{bmatrix} = \begin{bmatrix} \Delta\boldsymbol{\tau} \\ \mathbf{0} \end{bmatrix} \tag{4}$$

or in a more compact form

$$\mathbf{M}(\boldsymbol{\theta})\Delta\ddot{\mathbf{q}} + \mathbf{K}\Delta\mathbf{q} = \mathbf{L}\Delta\boldsymbol{\tau} \tag{5}$$

where

$$\Delta\mathbf{q} = \begin{bmatrix} \boldsymbol{\theta} \\ \Delta\mathbf{e} \end{bmatrix}$$

$$\Delta\mathbf{e} = \mathbf{e} - \mathbf{e}_0 = \mathbf{e} + \mathbf{K}_{22}^{-1}\mathbf{g}_2(\boldsymbol{\theta})$$

$$\Delta\boldsymbol{\tau} = \boldsymbol{\tau} - \mathbf{g}_1(\boldsymbol{\theta})$$

Inverting the inertia matrix at a given configuration $\boldsymbol{\theta}$ we obtain

$$\begin{bmatrix} \ddot{\boldsymbol{\theta}} \\ \Delta\ddot{\mathbf{e}} \end{bmatrix} = -\mathbf{M}^{-1}\begin{bmatrix} \mathbf{0} & \mathbf{0} \\ \mathbf{0} & \mathbf{K}_{22} \end{bmatrix} \begin{bmatrix} \boldsymbol{\theta} \\ \Delta\mathbf{e} \end{bmatrix} + \mathbf{M}^{-1}\begin{bmatrix} \mathbf{I}_{n\times n} \\ \mathbf{0} \end{bmatrix}\Delta\boldsymbol{\tau} \tag{6}$$

The lower part of this equation expresses the relationship between $\Delta\mathbf{e}$ and $\Delta\boldsymbol{\tau}$ and therefore can be used to study the controllability of the elastic deformations.

Denoting

$$\mathbf{M}^{-1} = \begin{bmatrix} (\mathbf{M}^{-1})_{11} & (\mathbf{M}^{-1})_{12} \\ (\mathbf{M}^{-1})_{21} & (\mathbf{M}^{-1})_{22} \end{bmatrix} \tag{7}$$

the relation between $\Delta\mathbf{e}$ and $\Delta\boldsymbol{\tau}$ can be written as

$$\Delta\ddot{\mathbf{e}} = -(\mathbf{M}^{-1})_{22}\mathbf{K}_{22}\Delta\mathbf{e} + (\mathbf{M}^{-1})_{21}\Delta\boldsymbol{\tau} \tag{8}$$

and transforming this equation to the state-space we have

$$\begin{bmatrix} \Delta\ddot{\mathbf{e}} \\ \Delta\mathbf{e} \end{bmatrix} = \begin{bmatrix} \mathbf{0} & -(\mathbf{M}^{-1})_{22}\mathbf{K}_{22} \\ \mathbf{I}_{m\times m} & \mathbf{0} \end{bmatrix} \begin{bmatrix} \Delta\dot{\mathbf{e}} \\ \Delta\mathbf{e} \end{bmatrix} + \begin{bmatrix} (\mathbf{M}^{-1})_{21} \\ \mathbf{0} \end{bmatrix}\Delta\boldsymbol{\tau} \tag{9}$$

or in a more compact form

$$\dot{\mathbf{z}} = \mathbf{A}\mathbf{z} + \mathbf{B}\Delta\boldsymbol{\tau} \tag{10}$$

where

$$\mathbf{z} = \begin{bmatrix} \Delta\dot{\mathbf{e}} \\ \Delta\mathbf{e} \end{bmatrix}$$

Then, the vibration controllability matrix $\mathbf{G}_c$ at a given configuration $\boldsymbol{\theta}$ is

$$\mathbf{G}_c(\boldsymbol{\theta}) = [\mathbf{B} \quad \mathbf{AB} \quad \ldots \quad \mathbf{A}^{2m-1}\mathbf{B}] \tag{11}$$

If rank $\mathbf{G}_c < 2m$ some structural vibrations are uncontrollable.

3 Control Algorithm

In this section, we introduce the control algorithm that was used to study the closed-loop behaviour of the example at the uncontrollable configurations. For further information see our previous papers (López-Linares et al., 1994).

The experimental robot FLEBOT II uses hardware velocity servo loops that can be written as

$$\boldsymbol{\tau} = \boldsymbol{\Lambda}(\dot{\boldsymbol{\theta}}_c - \dot{\boldsymbol{\theta}}) \tag{12}$$

where $\boldsymbol{\Lambda}$ is the diagonal matrix of servo gains and $\dot{\boldsymbol{\theta}}_c$ is the vector of velocity commands. Introducing Eq. (12) into Eq. (5) and making the approach $\boldsymbol{\Lambda}\dot{\boldsymbol{\theta}}_c - \mathbf{g}_1(\boldsymbol{\theta}) \approx \boldsymbol{\Lambda}\dot{\boldsymbol{\theta}}_c$ (the servo gains are assumed to be high), the dynamic equation of the robot + servo system is

$$\mathbf{M}(\boldsymbol{\theta})\Delta\ddot{\mathbf{q}} + \mathbf{L}\boldsymbol{\Lambda}\mathbf{L}^t\Delta\dot{\mathbf{q}} + \mathbf{K}\Delta\mathbf{q} = \mathbf{L}\boldsymbol{\Lambda}\dot{\boldsymbol{\theta}}_c \tag{13}$$

A software velocity control law can be obtained for the robot in the form

$$\dot{\boldsymbol{\theta}}_c = -\mathbf{F}pr(\boldsymbol{\theta} - \boldsymbol{\theta}_d) - \mathbf{F}_{it}\int_0^t (\boldsymbol{\theta} - \boldsymbol{\theta}_d)dt - \mathbf{F}_{pe}(\boldsymbol{\theta})\Delta\mathbf{e} - \mathbf{F}_{ie}(\boldsymbol{\theta})\int_0^t \Delta\mathbf{e}dt \tag{14}$$

where the gains $\mathbf{F}pt$ and $\mathbf{F}it$ are diagonal matrices and the gains $\mathbf{F}_{pe}$ and $\mathbf{F}_{ie}$ are obtained from the solution of an optimal control problem.

We can study the closed-loop behaviour of the robot from Eqs. (13) and (14). For each vibration mode there is a corresponding pair of closed-loop poles and the real part of these poles becomes zero at the configurations where it cannot be controlled. Thus, the closed-loop poles give us not only the configurations where the vibrations are uncontrollable, but also which mode is uncontrollable. See the case study in Section 4.4.

4 Example of a 3D Flexible Manipulator

In this section we numerically study the controllability of the flexible robot FLEBOT II built at the Department of Aeronautics and Space Engineering of Tohoku University; and in the next section we present the experimental results.

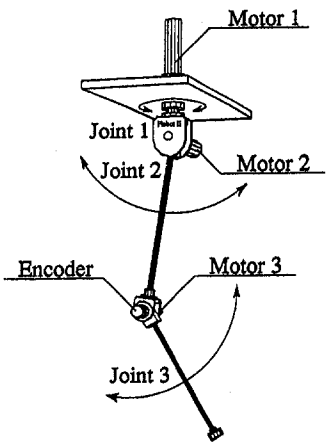

Fig. 1 Overview of the experimental flexible manipulator FLEBOT II

Table 1 Properties of FLEBOT II

Parameter	Notation	Value
Length of the links	l_2 [m]	0.50
	l_3 [m]	0.44
Stiffness of the links	E_2I_2 [Nm^2]	41.82
	E_3I_3 [Nm^2]	13.23
Torsional stiffness	G_2J_2 [Nm^2]	32.17
	G_3J_3 [Nm^2]	10.18
Mass of the joints	m_2 [kg]	1.5
	m_3 [kg]	0.3
Reduction ratios	R_1	100
	R_2	100
	R_3	88
Actuators' inertia	I_{a_1} [kgm^2]	0.326
	I_{a_2} [kgm^2]	0.326
	I_{a_3} [kgm^2]	0.041
Servo gains	Λ_1 [Nms/rad]	150.7
	Λ_2 [Nms/rad]	150.7
	Λ_3 [Nms/rad]	38.9

4.1 Laboratory Setup. Figure 1 shows an overview of FLEBOT II. It can be seen that the robot is composed of two elastic rods and three motors (DC type).

Each motor is connected to a Harmonic Drive and is controlled by a hardware velocity servo card using tachometer feedback. Encoders are employed to measure joint rotations and strain gages located at the root of each rod permit to measure the elastic deflections.

A 486 personal computer processes the information given by the sensors and calculates the velocity commands to control the movement of the joints.

4.2 Lumped-Mass Model. Assumming that the links are massless slender beams, a technique based on the Holzer's Method (Konno and Uchiyama, 1996) can be applied to obtain a lumped-mass model of FLEBOT II.

Figure 2 shows a scheme of this model which has 7 coordinates: 3 joint rotations θ_1, θ_2, θ_3 and 4 elastic deflections δ_{y_2}, δ_{z_2}, δ_{y_3}, δ_{z_3}. The robot mechanism can be defined by the actuators' inertias I_{a_1}, I_{a_2}, I_{a_3}, the reduction ratios R_1, R_2, R_3, the length of the links l_2, l_3, the concentrated masses at the tip of the links m_2, m_3 and the elastic and torsional properties of the links, E_2I_2, E_3I_3 and G_2J_2, G_3J_3 respectively. The actuators' servo loop can be defined by the servo gains Λ_1, Λ_2 and Λ_3. Table 1 lists the values of the properties of FLEBOT II.

In the case of the 2-link 3-joint flexible manipulator the general Eq. (5) can be decoupled into two separate equations as follows

$$\mathbf{M}_h(\boldsymbol{\theta})\Delta\ddot{\mathbf{q}}_h + \mathbf{K}_h\Delta\mathbf{q}_h = \mathbf{L}_h\Delta\boldsymbol{\tau}_h \tag{15}$$

$$\mathbf{M}_\nu(\boldsymbol{\theta})\Delta\ddot{\mathbf{q}}_\nu + \mathbf{K}_\nu\Delta\mathbf{q}_\nu = \mathbf{L}_\nu\Delta\boldsymbol{\tau}_\nu \tag{16}$$

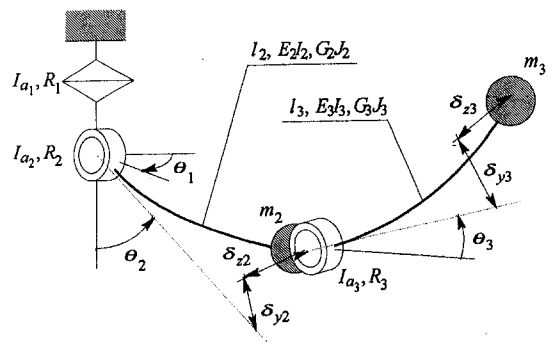

Fig. 2 Lumped mass model of FLEBOT II

where

$$\Delta\mathbf{q}_h = \begin{bmatrix} \theta_1 \\ \Delta\delta_{z_2} \\ \Delta\delta_{z_3} \end{bmatrix}, \quad \Delta\mathbf{q}_\nu = \begin{bmatrix} \theta_2 \\ \theta_3 \\ \Delta\delta_{y_2} \\ \Delta\delta_{y_3} \end{bmatrix}$$

$$\Delta\boldsymbol{\tau}_h = [\Delta\tau_1], \quad \Delta\boldsymbol{\tau}_\nu = \begin{bmatrix} \Delta\tau_2 \\ \Delta\tau_3 \end{bmatrix}$$

- On the one hand, the subsystem indicated by subscript ν is related to the movement and deflections of the robot in the vertical plane determined by the angle θ_1 and will be called the "vertical subsystem."
- On the other hand, the subsystem indicated by subscript h is related to the rotation θ_1 and the deflections normal to the vertical plane and will be called the "horizontal subsystem."

We have studied the controllability of both, but as the vertical subsystem is controllable we are going to concentrate in this paper on the study of the horizontal subsystem. In this subsystem the gravity terms are equal to zero, and therefore $\Delta\mathbf{e}_h = \mathbf{e}_h$ and $\Delta\boldsymbol{\tau}_h = \boldsymbol{\tau}_h$ (see Eq. (5)).

4.3 Vibration Controllability of the Horizontal Subsystem. Applying the method described in Section 2 to the horizontal subsystem, we find that the vibration controllability matrix $\mathbf{G}_c(\boldsymbol{\theta})$ depends only upon θ_2 and θ_3. To study the controllability we must study the rank of $\mathbf{G}_c(\theta_2, \theta_3)$ in all the configurations.

Figure 3 plots the minimum singular value of the controllability matrix for $0 < \theta_2 < \pi$, $0 < \theta_3 < \pi$. The configurations in which the minimum singular value is equal to 0 are the uncontrollable configurations or the singular lines of controllability.

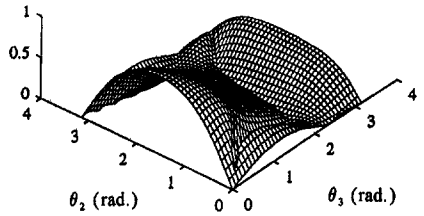

Fig. 3 Minimum singular value of the controllability matrix

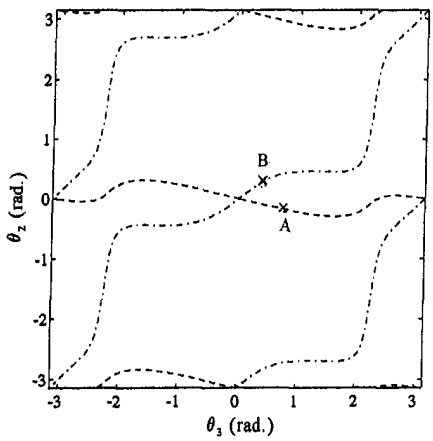

Fig. 4 Complete map of singular lines

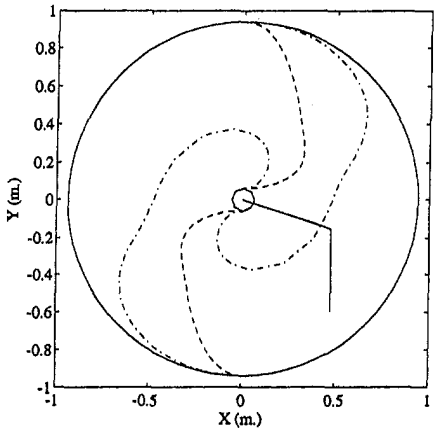

Fig. 6 Controllable subspaces for $\theta_3 < 0$

Figure 4 plots the complete map of these lines. It can be seen that it is only necessary to study the controllability in the range $0 < \theta_2 < \pi$, $0 < \theta_3 < \pi$ because of the symmetry of the picture.

4.4 Closed-Loop Poles. From Eqs. (13) and (14) it is possible to study the closed-loop behavior of the horizontal subsystem at the singular lines. Using the same technique as in a previous work (Lopez-Linares et al., 1994) we have computed the pairs of poles related to the first and second vibration modes in the range $0 < \theta_2 < \pi$, $0 < \theta_3 < \pi$, and we plot their real parts in Fig. 5.

It can be seen that the real parts become zero at some configurations. These configurations coincide with the ones that we obtained from the vibration controllability matrix: the zeros of Figs. 5(a) and 5(b) give us the dashed lines and the dashdot lines of Fig. 4, respectively.

Therefore, from the closed-loop poles we can interpret the meaning of the lines in Fig. 4: the dashed lines indicate the configurations where the first vibration mode is uncontrollable and the dashdot lines indicate the configurations where the second vibration mode is uncontrollable.

4.5 Controllable Subspaces. It is interesting to draw the singular lines in the robot's workspace. Considering $\theta_3 < 0$ we have 4 singular lines. For each pair (θ_2^*, θ_3^*) defining a singular line, there is a corresponding position (x^*, y^*) of the end-effector in the vertical plane determined by θ_1. Figure 6 plots the Cartesian singular lines (x^*, y^*) in the vertical plane. The solid lines show the limits of the workspace and the sketch of the robot in an arbitrary position. The dashed lines and the dashdot lines indicate the impossibility of controlling either the first or the second vibration mode respectively. It can be seen that the singular lines divide the workspace of FLEBOT II into four controllable subspaces.

The meaning of this picture is that we can control all the vibrations of the "horizontal motion," only when the tip of the robot is inside one subspace. If we apply a "vertical motion" to change from one subspace to another while we are moving the robot "horizontally" then, at some point of the movement, the tip of the robot will meet one of the singular lines of Figure 4, and the control algorithm will not be able to damp the corresponding vibration mode. However, if we only move "vertically," the horizontal modes will not be excited, and we can change of subspace with no vibrations.

5 Experimental Results

In order to check the validity of our simulations and to understand better the difficulties introduced by the uncontrollable configurations in the design of control algorithms for flexible robots, we have conducted experiments of position stabilization and trajectory tracking around the singular lines of FLEBOT II.

Let us consider points A ($\theta_2 = -10$ deg, $\theta_3 = 41$ deg) and B ($\theta_2 = 13$ deg, $\theta_3 = 20$ deg) picked up from the neighborhood of the first and second vibration mode uncontrollable configurations (the dashed lines and the dashdot lines in Fig. 4, respectively).

Setting FLEBOT II at these two configurations and changing the reference position of θ_1 from 0 to 10 deg, we obtained the results plotted in Fig. 7. As expected, we can see that in point A the first mode cannot be controlled and in point B the same thing happens with the second mode. This instability is caused by the configuration-dependent uncontrollable nature of the robot, that causes the gain functions $\mathbf{F}_{pe}(\theta)$ and $\mathbf{F}_{ie}(\theta)$ to be discontinuous at the singular lines.

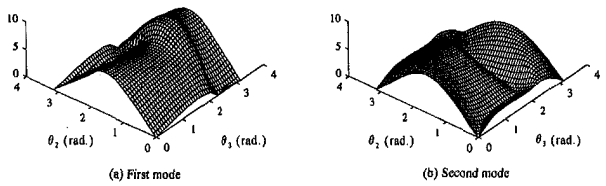

Fig. 5 Negative real parts of the closed-loop poles related to the vibration modes

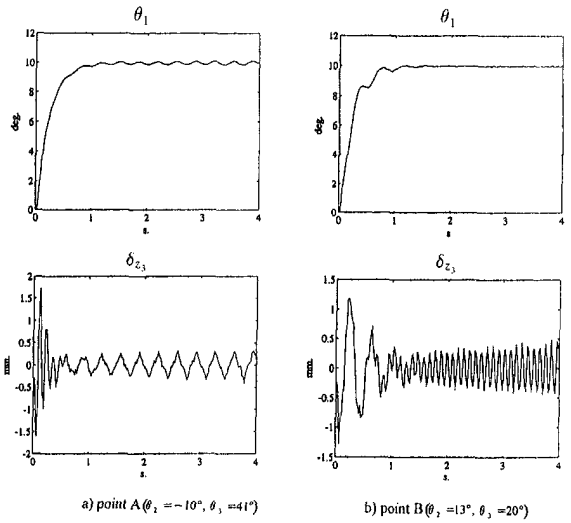

Fig. 7 Experimental step motion of 10 deg at points A and B (a) point A ($\theta_2 = -10$ deg, $\theta_3 = 41$ deg); (b) point B ($\theta_2 = 13$ deg, $\theta_3 = 20$ deg)

6 Conclusions

3D flexible robots may have uncontrollable configurations at which some of the vibration modes cannot be damped by the control law. We have given a method to find these configurations.

The concept of controllable subspaces (regions of the workspace where the vibrations can be controlled) seems to be interesting, in order to assure the suppression of vibrations in a practical application of a flexible robot.

In the case of the 2-link 3-joint flexible robot, the change from one-controllable subspace to another can be done with no vibrations by means of applying a vertical motion.

Acknowledgments

The authors would like to acknowledge the support of this work by the Mitsubishi Foundation, the Basque Government through its Education Department and others.

References

Balas, M. J., 1978, "Feedback Control of Flexible System," *IEEE Trans. on Automatic Control,* Vol. AC-23, No. 4, pp. 673–679.

Bayo, E., Papadopoulos, P., Stubbe, J., and Serna, M. A., 1989, "Inverse Dynamics and Kinematics of Multi-Link Elastic Robots: An Iterative Frequency Domain Approach," *Int. J. of Robotics Research,* Vol. 8, No. 6, pp. 49–62.

Book, W. J., 1984, "Recursive Lagrangian Dynamics of Flexible Manipulator Arms," *Int. J. of Robotics Research,* Vol. 3, No. 3, pp. 87–101.

Cannon, Jr., R. H., and Schmitz, E., 1984, "Initial Experiments on the End-Point Control of a Flexible One-Link Robot," *Int. J. of Robotics Research,* Vol. 3, No. 3, pp. 62–75.

Fukuda, T., 1985, "Flexibility Control of Elastic Robotic Arms," *J. of Robotic Systems,* Vol. 2, No. 1, pp. 73–88.

Khorrami, F., and Jain, S., 1992, "Experimental Results on an Inner/Outer Loop Controller for a Two-link Flexible Manipulator," *Proc. of the IEEE Int. Conf. on Robotics and Automation,* Vol. 2, pp. 742–747.

Konno, A., Uchiyama, M., Kito, Y., and Murakami, M., 1994, "Vibration Controllability of Flexible Manipulators," *Proc. of the IEEE Int. Conf. on Robotics and Automation,* San Diego, pp. 308–314.

Konno, A., and Uchiyama, M., 1996, "Modeling of a Flexible Manipulator Dynamics Based upon Holzer's Model," *Proc. of the Int. Conf. on Intelligent Robots and Systems (IROS),* Osaka, Japan, November 4–8 (to appear).

Kotnik, P. T., Yurkovich, S., and Özgüner, Ü., 1988, "Acceleration Feedback Control of a Flexible Manipulator Arm," *J. of Robotic Systems,* Vol. 5, No. 3, pp. 159–164.

López-Linares, S., Jacobus, R., Carrera, E., and Serna, M. A., 1991, "Inverse Dynamics Based Trayectory Tracking For a One-Link Flexible Arm," *Proc. of ASME Int. Conf. on Computers in Engineering,* pp. 543–548.

López-Linares, S., Konno, A., and Uchiyama, M., 1994, "Vibration Suppression Control of Flexible Robots Using Velocity Inputs," *Proc. of the Int. Conf. on Intelligent Robots and Systems (IROS),* Munich, Germany, pp. 1429–1437.

Sakawa, Y., Matsuno, F., and Fukushima, S., 1985, "Modeling and Feedback Control of a Flexible Arm," *J. of Robotic Systems,* Vol. 2, No. 4, pp. 453–472.

Siciliano, B., and Book, W. J., 1988, "A Singular Perturbation Approach to Control of Lightweight Flexible Manipulators," *Int. J. of Robotics Research,* Vol. 7, No. 4, pp. 79–90.

Tosunoglu, S., Lin, S. H., and Tesar, D., 1992, "Accessibility and Controllability of Flexible Robotic Manipulators," ASME JOURNAL OF DYNAMIC SYSTEMS, MEASUREMENT AND CONTROL, Vol. 114, pp. 50–58.

Uchiyama, M., Jiang, Z. H., and Hakomori, K., 1990, "Compensating Control of a Flexible Robot Arm," *Journal of Robotics & Mechatronics,* Vol. 2, No. 2, pp. 29–38.

Position Control of Single Link Flexible Manipulator by Variable Structure Model Following Control

S. Thomas[1] and B. Bandyopadhyay[1]

A variable structure model following controller (VSMFC) is designed for the tip position control of a single flexible link. The design is done for the system model in which only the first two flexible modes are included. Due to the simplicity in choosing second order models for the subsystems representing the dynamics of the various flexible modes, the design can be easily extended to include any desired number of flexible modes. The tip position response is made to assume a second order step response by suppressing the flexible modes very quickly. Hence the tip position response can be easily controlled by a suitable choice of the damping factor and natural frequency of the second order model which the rigid body mode of the link is made to follow. The controller is robust to parameter variations and disturbances.

1 Introduction

Various advantages of flexible links make them desirable to rigid links. But the flexibility of such links make the position controller design difficult because one has to control not only the rigid mode but also the highly vibratory modes. Theoretically, a flexible arm is an infinite order system. Designing a controller for a high-order system and implementing it may not be practically feasible. Hence a reduced order model is a prerequisite for the design of any practical controller. Owing to the fact that actuators and sensors cannot operate in the high frequency range, the flexible arm is approximated by finite models that consist of finite number of modes. But the controller designed should be such that the higher-order modes, that are not included in the model and hence not considered in controller design, are not excited.

Various control strategies for flexible links are reported in the literature such as robust control (Bontsema et al., 1988), pole placement method (Book and Majette, 1983), optimal control (Cannon and Schmitz, 1984), variable structure control (Qian and Ma, 1992) etc. Most of the control strategies when implemented in practice may not yield high performance due to uncertainty in model, parameter variations and disturbance effects. Even the variable structure control design by Qian and Ma (1992) does not offer invariance property to parameter variations and disturbance effects because the functional relationship of the tip position with the generalised co-ordinates of the system through the mode shape functions is not duely considered in the design procedure. This drawback has been pointed out by Thomas and Bandyopadhyay (1997). The VSMFC technique presented here not only guarantees invariance to a class of parameter variations and disturbances (Drazenovic, 1969) but also posses the other attractive features of variable structure systems (VSS).

Adaptive model following control (AMFC) has been proven to be superior to linear model following control because the former is capable of handling parameter variations and disturbances. AMFC technique, though capable of sending the steady state error to zero, fails to offer any quantitative control over the error transients (Hang and Parks, 1973; Landau, 1974; Narendra and Lin, 1980). Young (1977, 78) made use of the theory of VSS in designing AMFC system. Young's method not only produces asymptotically stable systems, but is also capable of prescribing the error transient. Young (1978) has designed an adaptive model following controller for a multivariable system where he employs the hierarchy of controls method

[1] Department of Electrical Engineering, IIT Bombay, Bombay—400076, India. S. Thomas is on deputation from Calicut Regional Engg. College, Calicut, Kerala—673601, India, B. Bandyopadhyay, currently as a Humboldt Fellow, is with the Lehrstuhl für Elektrische Steuerung und Regelung, Ruhr-Universität Bochum, Bochum 44780, Germany.

Contributed by the Dynamic Systems and Control Division of THE AMERICAN SOCIETY OF MECHANICAL ENGINEERS. Manuscript received by the DSCD March 1995. Associate Technical Editor: V. Utkin.